Asymptotic separation in multispecies collisional plasma shocks

C. Bellei and P. A. Amendt
Lawrence Livermore National Laboratory, 7000 East Avenue, Livermore, California 94550, USA
(Received 13 February 2014; published 2 July 2014)

When a piston drives a shock in a multicomponent plasma, residual separation of the ion species persists close to the piston-plasma boundary, long after the shock has propagated away from the boundary and has reached a (nearly) steady-state solution. This effect is observed in hybrid particle-in-cell simulations with two kinetic ion species and fluid electrons. It is a consequence of the different dynamics experienced by ions of different mass and charge-to-mass ratio and must be taken into account to properly model the physics of species separation in collisional plasma shocks.

DOI: 10.1103/PhysRevE.90.013101 PACS number(s): 52.57.−z, 52.50.Lp, 52.50.Jm

In 1960 Sherman conjectured that when a piston is accelerated in a binary mixture of neutral gases initially at rest, the heavier species is left behind so that there is a surplus of heavy molecules in the vicinity of the piston [1]. This mechanism was necessary in order to explain how the steady-state solution of a shock propagating in a binary mixture of gas molecules would predict a surplus of light molecules across the *whole* shock front, as also reported in Ref. [2], in apparent violation of conservation of total particle number. However, as Sherman [1] pointed out this paradox is resolved "at infinity", near the piston, where there should be a surplus of heavy molecules and conservation of the particle number would be restored.

It seems reasonable that this physical picture should also apply to the case of a plasma composed of two distinct ion species. Formally, the diffusion equation is the same as in a binary mixture of neutral gases, with the addition of a diffusive term driven by an electric field and potentially different temperatures for electrons and ions [3,4]. Typically the lighter species goes ahead of the heavy one [5], although there is the possibility that, when electrodiffusion dominates, the shock is richer in the species with the highest charge-to-mass ratio (since in most cases the species with the highest charge-to-mass ratio is also the lightest one; in this manuscript the term "light species" will be used in this loose sense).

Over time, the distance between the region richer in the heavy component and the one richer in the light component (the shock front) increases. In practice, the two regions are effectively decoupled when the distance from the piston to the shock front is on the order of an electron-ion thermalization length. At this point, the Rankine-Hugoniot jump conditions can be considered applicable to a good degree, though not exactly since the shock front is no longer completely localized.

It is the objective of this paper to study numerically this effect of "asymptotic separation" in a plasma, not just relying on a steady-state solution but also taking the transient regime into account. For this purpose, the case of interest is the one of a piston that drives a shock in a binary mixture of ions (and neutralizing electrons).

Interest in this problem originates in inertial confinement fusion (ICF) applications, where mixtures of different ion species routinely occur. In particular, the fuel composed of deuterium and tritium can be considered fully ionized during most of the implosion of the capsule. A plasma state is also reached in the ablator, which is usually made of some variant of plastics and thus contains a mixture of carbon and hydrogen ions.

The idea that appreciable species separation could occur during ICF implosions has been put forward only recently as a possible explanation for disagreements between experimental and simulation results [6]. Subsequent work seems to favor the idea that while species separation does indeed occur, especially during the converging stage of an implosion, it is reduced after shock rebound when the mean free paths become much smaller than the size of the hot spot [7]. Since research on this topic may still be considered at an early stage, there is room for basic studies and for a more fundamental understanding of species separation in a plasma that motivates this work.

A sketch of the expected solution of a shock-tube problem is shown in Fig. 1. As usual, concentration is defined as the ratio of the ion number density for the light species over the total ion number density. Ahead and immediately behind the shock, the concentration of the light species is equal to that of the undisturbed gas; departure from this value is only evident near the shock front and the piston boundary.

In the frame of the piston, the region near the piston itself reaches a zero-mean-velocity and zero-electric field within a few collision times, while the temperatures of the different ion and electron species relax to the same value within a few equilibration times.

In order to better understand the underlying physics, suppose that the two ion species are not interacting with each other, but only interacting with themselves (*intra*species collisions only are allowed). In this case, the result of a piston driving a shock could be sketched as in Fig. 2, where the heavier gas is left behind but is at a higher density. In the laboratory frame, the shock speed for the two (or more) noninteracting ion species follows the formula

$$v_{s,\alpha} = \frac{\gamma+1}{4} v_p + \left[\left(\frac{\gamma+1}{4} v_p \right)^2 + a_{0,\alpha}^2 \right]^{1/2}, \qquad (1)$$

where the subscript α denotes the ion species, γ is the specific heat ratio, v_p is the piston velocity, and $a_{0,\alpha} = \sqrt{(Z+1)\gamma k_B T/m_\alpha}$ is the speed of sound of the unperturbed gas with atomic number Z. Due to the dependence of $v_{s,\alpha}$ on the speed of sound, the shock is faster for the lighter component. However, the Mach number $M_\alpha = v_{s,\alpha}/a_{0,\alpha}$ of the shock is higher for the heavy species, consistent with the

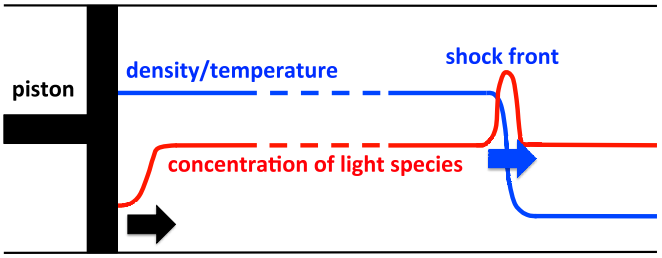

FIG. 1. (Color online) A piston suddenly accelerated in a binary mixture of neutral gases initially at rest generates a propagating shock. The shock front is enriched by the light species ("species separation"). Conservation of the total particle number is met by a deficit of light molecules near the piston.

higher jump in density. Hence, the temperature behind the shock will also be higher for the heavier species.

In order to look at this effect in detail, for the case of a plasma, simulations were performed with the hybrid particle-in-cell (PIC) code LSP [8]. The ion species were chosen to be deuterons and tritons, as these are of relevance in fusion research. The ions were treated kinetically, using a binary collision operator [9,10]. The electrons were treated as fluid particles, with the equation of state of an ideal gas. For the electron species, the flux limiter $f = 0.01$ was chosen to limit the electron heat flux to a fraction of the electron free-streaming flux. An implicit electromagnetic field solver was used.

In order to study the case of a shock driven by a piston, at $t = 0$ a charge- and current-neutral plasma flow was directed with a prescribed velocity against a perfectly reflecting wall. This method is the same as that used for the study of collisionless shocks in plasmas [11]. The wall is stationary in the simulation box; hence the problem at hand is equivalent to the case of a piston that drives a shock, as seen in the reference frame of the piston itself.

It is interesting to compare the case with noninteracting ions to the realistic case in which *inter* species collisions are allowed to occur.

For the noninteracting case, Fig. 3 was obtained from two separate one-dimensional simulations, with the objective of studying the behavior of the two ion species in the absence of the other species, i.e., as if interspecies collisions were not occurring. The parameters of the simulations were the following. For both cases, the length of the box was 8 cm with 6000 cells, implying a spatial resolution $\Delta x = 13\ \mu$m. There were 2500 ions per cell. The time resolution was $\Delta t = 90$ fs, a factor of 2 larger than the electromagnetic Courant limit but small enough to resolve all the collisions in the system. The temperature of the undisturbed gas was set to 100 eV and the particle density to 5×10^{20} cm^{-3} for each ion species. The velocity of the flow directed against the wall was $v/c = 2.3 \times 10^{-3}$, resulting in the Mach number $M = 7.4$ (temperature behind the shock of 1.8 keV) for the deuteron case and $M = 8.8$ for the triton case (temperature behind the shock of 2.5 keV).

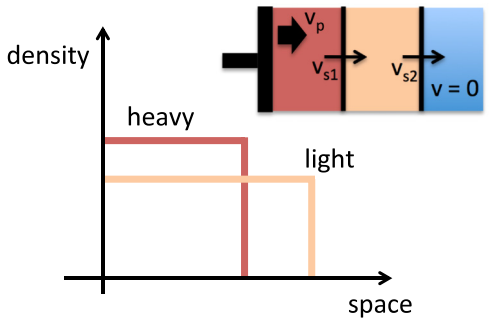

FIG. 2. (Color online) A system of two noninteracting ion species behaves as sketched in this figure: the shock of the lighter ion is faster than the one of the heavy one. The heavy ions are left behind, at a higher peak density.

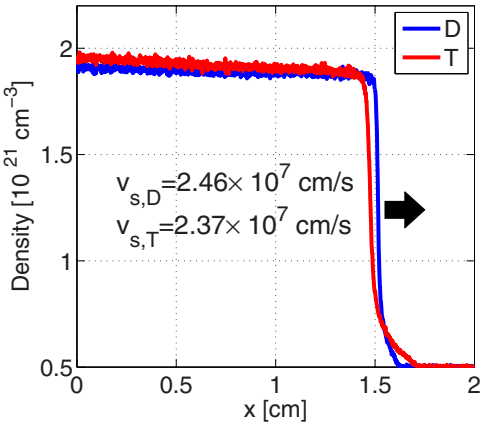

FIG. 3. (Color online) Number density for the deuterons and tritons, accelerated from a piston with velocity $\beta = 2.3 \times 10^{-3}$. This figure was obtained from two *separate* simulations, one with D ions and the other one with T ions, in order to show the case of noninteracting gases.

As expected from the previous discussion, the deuteron (D) shock is faster than the triton (T) shock but the density of the T ions is larger. In the piston frame (i.e., the frame of the simulation), a linear fit of the shock position vs time results in shock speeds of 2.46×10^7 and 2.37×10^7 cm/s, respectively. These values are within 0.5% of those obtained from Eq. (1), once the simulated shock velocities are transformed into the laboratory frame.

Despite the shock speed being larger for the deuterons, the width of the shock is larger at the triton shock front, due to the dependence of the ion-ion mean free path on the square of the temperature. In fact, in Fig. 3 the pedestal of the red curve is actually ahead of the blue curve; however, at later times the D shock will completely overtake the T shock.

The next level of complication consists of the inclusion of interspecies collisions, which has the effect of substantially limiting the separation between species.

Some of the parameters of this simulation were different from those of the noninteracting cases: the box length was reduced to 3 cm and the number of cells was 3000, giving a spatial resolution of $\Delta x = 10\ \mu$m. The time resolution was $\Delta t = 100$ fs. The other parameters were kept the same. The resulting Mach number of the combined shock was $M = 8.2$, close to the mean of the separate D and T shocks.

As soon as the incoming flow of the two (now interacting) ion species reflects from the wall, particles start

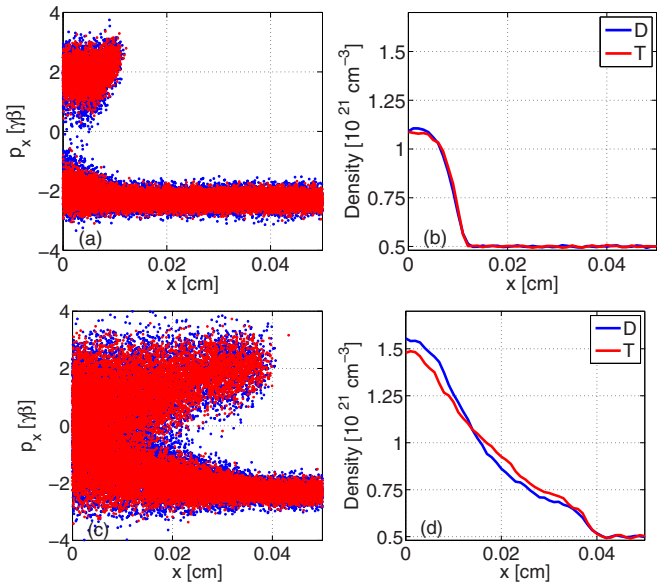

FIG. 4. (Color online) Early stages of a hybrid PIC simulation for a piston traveling with normalized velocity $\beta = 2.3 \times 10^{-3}$ in a mixture of interacting D and T ions. The panels show the phase space of the two ion species [panels (a) and (c)] and the corresponding number density [panels (b) and (d)]. Top row: $t = 0.15$ ns. Bottom row: $t = 0.55$ ns.

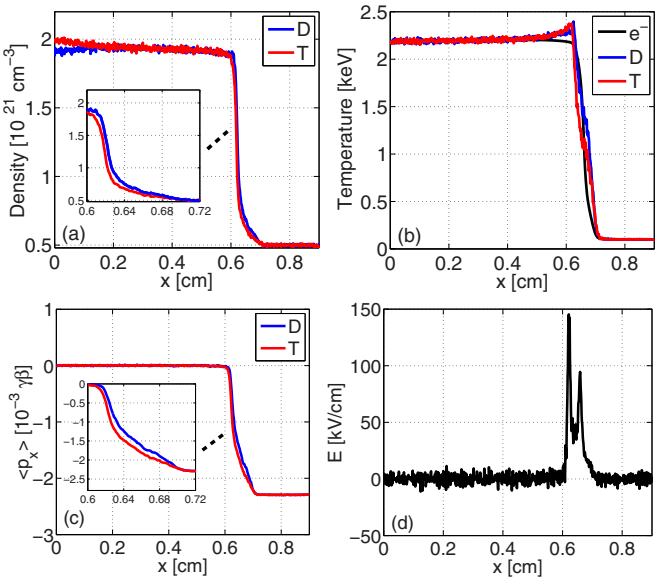

FIG. 5. (Color online) Steady-state solution of the same problem presented in the previous figure. The different panels display (a) number density, (b) temperature, (c) average longitudinal momentum, and (d) electric field at the time $t = 26$ ns.

counterstreaming near the wall region. Initially, for times that are shorter than a collisional mean free time, the system behaves nearly as a collisionless plasma. As is apparent from Fig. 4(a), in this transient regime the phase space near $p_x = 0$ is devoid of particles and the density is nearly $2\times$ the initial density, implying that there is simple beam overlapping, as shown in the density plot in Fig. 4(b). With time, collisions start populating the region at $p_x = 0$ and the density asymptotes to its downstream Rankine-Hugoniot value behind the shock, $n \simeq 3.83\, n_0 = 1.9 \times 10^{21}$ cm^{-3}.

In the transient regime, the lighter deuterons respond more rapidly to the sudden acceleration of the piston and their density is slightly larger than the triton density [Figs. 4(b) and 4(d)]. The reason for this may lie in the details of the distribution function for the different species and in the strong dependence of the Coulomb cross section on the velocity difference between two encounters. More specifically, since the velocity spread of the distribution function depends on the ion mass as $1/\sqrt{m_i}$, there is a larger overlap of the tails of the incident and reflected beams for lower masses, with the result that the phase space near $p_x = 0$ is filled more efficiently for the lighter species.

Several plots when the simulation reaches a steady state are shown in Fig. 5. The electric field shows a double peak, in agreement with the fluid theory for strong shocks [12]. At this stage, there is a surplus of tritons close to the piston wall at $x = 0$ (red line). The plots of temperature, velocity, and electric field show that the region near the wall is essentially at rest and has equilibrated and that there is no electric field present. The only dynamics that can occur in this region is due to gradients in concentration, which will asymptotically decrease over time due to diffusion. Since classical diffusion is essentially a random walk process, the velocity at which gradients near the wall will spread in time is $\propto 1/\sqrt{\text{time}}$. By contrast, the speed of the shock is constant once a steady state is reached. Hence, the distance between the region richer in T ions (piston) and the one richer in D ions (shock front) increases with time. In practice, this means that, when using a moving window numerical technique in order to follow a shock, the number of particles inside the moving window is not conserved during the transient phase.

The separation between D and T ions that is found in these simulations can be compared with the result obtained when an average ⟨DT⟩ species is used. The density of the average species is chosen so as to conserve both total density and particle number [13], so that initially $\rho_{\langle \mathrm{DT}\rangle} = \rho_1 + \rho_2$ and $n_{\langle \mathrm{DT}\rangle} = n_\mathrm{D} + n_\mathrm{T}$. Also, the mass of the average species is chosen as $m_{\langle \mathrm{DT}\rangle} = \alpha_1 m_1 + \alpha_2 m_2$, where α_1 and α_2 represent the number concentration of the two species. Since in these simulations an equimolar mixture of D and T ions is assumed, it follows that $m_{\langle \mathrm{DT}\rangle} = (m_1 + m_2)/2$.

Figure 6 compares the number density and temperature obtained in these two cases, where the two-species calculation is the same as the one shown in Fig. 5. The density of the ⟨DT⟩ calculation lies in between the solution obtained when the deuterons and tritons are treated as distinct, but interacting, species.

The ⟨DT⟩ calculation clearly cannot capture all the dynamics of a two-ion-species calculation. To what extent this matters for achieving ignition in ICF implosions is the subject of ongoing research and debate. In Fig. 7, the work done by the piston in compressing the plasma electrons and ions is shown as a function of time, for the same two cases. The energy to compress the fluid electrons is calculated as

$$W_e(t) = \int_\Omega \left[c_v(\rho_e T_e - \rho_{e,0} T_{e,0}) + \frac{1}{2}\rho_\mathrm{e}(u_e - u_{e,0})^2 \right] d\Omega,$$

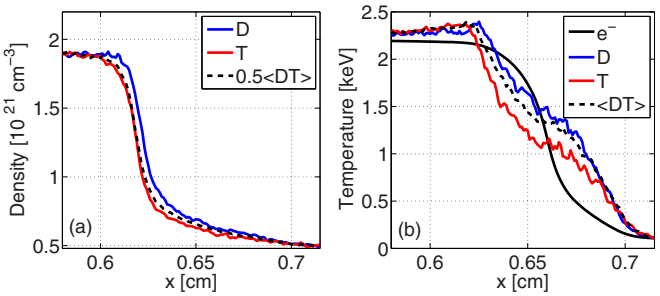

FIG. 6. (Color online) Comparison of solutions for a two-species and an average-species calculations. (a) Number density (the average-species calculation is divided by a factor 2 for comparison). (b) Temperature profiles. Only one curve is shown for the electron temperature, because the result was almost identical for the two simulations.

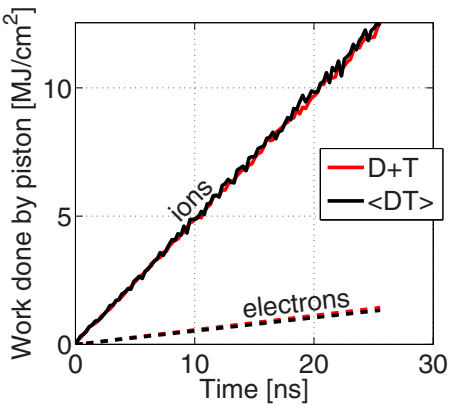

FIG. 7. (Color online) Work done on the ion and electron species by the piston, as a function of time. The red curves refer to the two-ion-species calculation and the black curves to the average-species calculation.

where c_v is the specific heat capacity at constant volume, T_e is the electron temperature, ρ_e is the electron density, and u_e is the electron velocity in the simulation (piston) frame. The subscript 0 denotes the initial value, with $-u_{e,0}$ being the piston velocity in the laboratory frame, and the integration is over a volume Ω that contains the shocked electrons at all times.

For the kinetic ions, the velocity of each particle is transformed into the laboratory frame and then the kinetic energy is summed over all the particles. Denoting by $\mathbf{p}_j$ the three-dimensional ion momentum in the simulation frame and by $\mathbf{p}_0$ the initial momentum, the resulting work performed by the piston on the ions is then

$$W_i(t) = \sum_\alpha \sum_j N_j |\mathbf{p}_j - \mathbf{p}_0|^2/2m_j, \qquad (2)$$

where the summation is over the species α and particles j within the volume Ω, the number of real particles per simulated particle is denoted by N_j, and the ion mass is denoted by m_j. For a Maxwell-Boltzmann distribution and in the continuum limit, Eq. (2) gives the expected fluid result that the average energy $\mathcal{E}$ per ion of mass m_i that is accelerated by the piston to a velocity $|\mathbf{p}_0|^2/2m_i$ is $\mathcal{E} = 3/2k_BT + |\mathbf{p}_0|^2/2m_i$. For completeness, the work done to build the electric field E should also be added, $W_E = \frac{1}{2}\int \varepsilon_0 E^2 d\Omega$, but this is negligible in comparison with W_e and W_i.

In both simulations, the total energy was conserved to better than the 99% level. As seen in Fig. 7, the work done by the piston appears to be very similar for the two-ion-species and average-species cases. Whether it should be virtually the same, or whether the small differences that are observed have a deeper meaning, is left for future studies.

It is important to note that the argument presented in this paper has a much more general validity than for the simple shock-tube problem here proposed: whenever a steady-state shock solution is reached, the shock front will *always* be richer in one of the two (or more) ion components. It follows necessarily that a surplus of the other component must be present somewhere else in the problem. To further elucidate this concept, it is useful to recall the simulations shown in Refs. [5,14]. In those simulations, the shock was produced in a Riemann-type problem, which includes the generation of a shock wave, a rarefaction wave, and a contact discontinuity. It is apparent by looking at the figures in the cited papers that, while the shock is richer in the light component, the rarefaction wave is richer in the heavy component. This is also due to the fact that sound waves travel faster in a lighter gas.

In summary, in this article the mechanism of "asymptotic separation" between different species is studied in the context of a binary mixture of ions in a neutralized plasma. The residual separation of the heavy component close to the piston-plasma boundary is produced in the initial stages of the simulations (the transient regime) and persists *ad infinitum*, even after the shock has reached a steady solution (in the frame of reference of the shock). This work serves as a basis to better understand and correctly model species separation, a topic that has recently gained interest in the context of ICF implosions.

The authors acknowledge useful discussions with S. C. Wilks. Computing support for this work came from a LLNL Computational Directorate Grand Challenge award. This work was performed under the auspices of the US Department of Energy by the Lawrence Livermore National Laboratory under Contract No. DE-AC52-07NA27344 and supported by LDRD-11-ERD-075.

[1] F. S. Sherman, J. Fluid Mech. **8**, 465 (1960).
[2] Ya. B. Zel'dovich and Yu. P. Raizer, *Physics of Shock Waves and High-Temperature Hydrodynamic Phenomena* (Dover, Mineola, New York, 2002).
[3] P. Amendt, C. Bellei, and S. Wilks, Phys. Rev. Lett. **109**, 075002 (2012).
[4] G. Kagan and X.-Z. Tang, Phys. Plasmas **19**, 082709 (2012).

[5] C. Bellei, P. A. Amendt, S. C. Wilks, M. G. Haines, D. T. Casey, C. K. Li, R. Petrasso, and D. R. Welch, Phys. Plasmas **20**, 012701 (2013).
[6] P. Amendt, S. C. Wilks, C. Bellei, C. K. Li, and R. D. Petrasso, Phys. Plasmas **18**, 056308 (2011).
[7] O. Larroche, Phys. Plasmas **19**, 122706 (2012).
[8] D. R. Welch, D. V. Rose, B. V. Oliver, and R. E. Clark, Nucl. Instrum. Methods Phys. Res., Sect. A **464**, 134 (2001).
[9] T. Takizuka and H. Abe, J. Comput. Phys. **25**, 205 (1977).
[10] K. Nanbu, Phys. Rev. E **55**, 4642 (1997).
[11] D. W. Forslund and C. R. Shonk, Phys. Rev. Lett. **25**, 1699 (1970).
[12] M. Y. Jaffrin and R. F. Probstein, Phys. Fluids **7**, 1658 (1964).
[13] C. Bellei, H. Rinderknecht, A. Zylstra, M. Rosenberg, H. Sio, C. K. Li, R. Petrasso, S. C. Wilks, and P. A. Amendt, Phys. Plasmas **21**, 056310 (2014).
[14] C. Bellei, P. A. Amendt, S. C. Wilks, D. T. Casey, C. K. Li, R. Petrasso, and D. R. Welch, Phys. Plasmas **20**, 044701 (2013); **20**, 044702 (2013).